A. Fredholm and J.L. Strudel

Ecole des Mines de Paris, Centre des Matériaux. B.P. 87 - 91003 EVRY Cédex France

#### Summary

Single crystals of  $\gamma'$  hardened nickel base superalloys of several compositions were grown along the <001> direction. Controlled thermal treatments led to a fairly regular distribution of <001> oriented  $\gamma'$  cuboïdal precipitates of about 0.4  $\mu m$  in size prior to creep tests at 1050°C under uniaxial tensile stress along the growth axis. Other specimens were aged for several hundred hours at 1050°C under no stress.

The lattice misfit parameter has been evaluated by TEM observations for several alloys. The density of equilibrium interfacial dislocations was taken as a good estimate of the in situ value of  $\delta$  at high temperature. Unstressed specimens heat-treated at 1050°C and rapidly quenched were observed. Alloys with significant values of the misfit parameter seem to exhibit excellent creep resistance at high temperature when a high volume fraction of the  $\gamma'$  phase is retained.

Coalescence of the  $\gamma'$  phase was examined under creep conditions after various creep times. Longitudinal cross sections of the specimens, examined by SEM, show plates and islands of  $\gamma$  and  $\gamma'$  phases. A careful examination of the morphology of each phase seems to indicate that the optimal creep resistance is obtained for alloys where the  $\gamma$  phase, initially surrounding the  $\gamma'$  particles, eventually becomes surrounded by it when oriented coalescence proceeds under creep conditions. Dislocation structures in both phases have been examined by TEM on cross sections normal to the stress axis. Deformation modes have been identified and are discussed in relation with purely elastic models describing oriented coarsening of the  $\gamma'$  phase.

## Introduction

The main source of hardening in nickel base single crystals used as turbine blades is provided by the  $\gamma'$  phase, an ordered phase of the type Ni<sub>3</sub>Al with L1 structure dispersed in an FCC matrix. In recent years new alloys have appeared presenting even higher volume fractions of the  $\gamma'$  phase: near 70% at room temperature and up to 750°C, and retaining still more than 50% of the hardening phase at 1050°C. The strength of these alloys designed for high temperature creep resistance is derived not only from the large volume fractions of the  $\gamma'$  phase they contain but also from their composition together with that of the matrix; it is also affected by the amplitude of the misfit parameter between the two phases  $\delta$ , the difference in elastic constants, anisotropy and  $\gamma/\gamma'$  interfacial energy.

One important source of concern of the last 10 years has been the tendency for the  $\gamma'$  phase to coalesce into larger precipitates at high temperature. Ostwald ripering is observed on populations of precipitates of small size (<100 nm) (1) but may be disturbed by the development of interfacial dislocation networks for larger sizes (2). Direct observation of quenched—in interfacial dislocation networks formed during long time annealing provides a simple method for measuring in situ misfit parameters at high temperature and has not been used extensively so far. A few estimates are presented in this paper and compared with room temperature measurements.

Directional coarsening of the  $\gamma'$  phase in the presence of an applied stress has been reported for various alloys (3-7). The most commonly observed morphology is the formation of "platelets" or "rafters" extending in the direction normal to the applied stress (3, 5) and referred to as type N later in this text. It is usually associated with negative values of & (4,5) although in U-700 a slightly positive parameter difference is reported at room temperature (8). The formation of "rods" or "platelets" elongated in the direction parallel to the applied stress and later referred to as type P has been observed in Ta rich nickel alloys by Carry and Strudel (7) and in the simple binary system Ni-Al by Miyasaki et al (6). The misfit parameter of the γ' phase appears to remain positive even at high temperature in these alloys. Other factors such as the ratio of the elastic moduli of the two phases E, /E the volume fraction of  $\gamma^{\prime}\text{,}$  the anisotropy factors, the  $\gamma/\gamma^{\prime}$  interfacial energy and the plastic deformation modes are likely to play a major role in determining the type of coalescence observed in an alloy at high temperature. Some of these points will be discussed in this paper.

### Experimental Procedure

Single crystals of three different alloys were grown by a seeded Bridgman technique with a withdrawal rate of 6cm/h: previously studied alloy 01 (7), a commercial alloy CMSX-2 and a Ta rich experimental alloy with high volume fraction of  $\gamma^{\prime}$ . The crystallographic orientation of specimens selected for creep tests laid within 7° of the [001] direction. After solutionizing at 1315°C for 3h alloy CMSX-2 and at 1290°C for 6h the experimental alloy, samples were given a 1h precipitation treatment at 1150°C (oil quench) followed by a complementary treatment of 16h at 870°C. Samples were creep tested under tensile constant load of 140 MPa at 1050°C in air. Most tests were carried out to failure, others were interrupted by forced air quenching under load after 1h and 100h creep respectively.

In order to observe interfacial dislocation networks and obtain a reasonable estimate of the  $\gamma-\gamma'$  misfit parameter at temperature, prolonged ageing was carried out at 1050°C for 100h (alloy 01), 200h (experimental

alloy) and 300h (CMSX-2) respectively after the full solutionizing treatment. Thus  $\gamma'$  precipitates larger than 1 $\mu m$  could be observed by TEM in each alloy.

Thin foils for TEM were prepared by mechanical grinding down to 0,15 mm followed by jet electro-polishing at 5°C in a 10 perchloric acid-45 acetic acid solution in butoxyethanol. Observations were carried out on a Philips EM 300 operating at 100 kV or on a Philips 430 operating at 300 kV.

The amplitude of the misfit parameter was estimated from the interfacial dislocation spacing by the method described by Lasalmonie and Strudel (2), correcting for the orientation of the plane of the interface with respect to the plane of observation. The sign of  $\delta$  was determined by imaging the dislocations under kinematical conditions (deviation parameter w > 0) under the  $\vec{g}$  parallel to  $\vec{b}$  condition. First  $\vec{b}$  was identified and then the  $\vec{g},\vec{b}=2$  condition was set in order to obtain asymetric images with the strong image appearing at wx > 0 (for  $\vec{g},\vec{b}>0$ ) when  $0_{7}$  is taken in the direction of the incident electron beam and  $0_{V}$  along the dislocation line  $(\vec{u})$ .

# Experimental Results

The microstructure of all alloys after full heat treatment is similar to that of figure 1 showing a [001] foil of the experimental alloy observed by dark field TEM with a superlattice spot. The  $\gamma'$  precipitates appear as cuboïds of about 0,4  $\mu$ m separated by thin walls of the  $\gamma$  matrix (10 to 30nm) and aligned along the cube directions in order to minimize elastic strain energy. A few precipitates of about 50 nm are visible in the wider regions of the  $\gamma$  matrix and seem to form during the last stage of the heat treatment (870°C/16h).

A typical tensile creep curve for these alloys at  $1050\,^{\circ}\text{C}$  under 140MPa is shown on figure 2, with 90% of the total plastic strain taking place during the last 10 h of the test.

# Microstructural Observations of Creep Tested Specimens

Three stages in the creep life of the experimental alloy were examined : after 1h (A on fig. 2), after 100h (stage B) and after rupture (stage C, 330h).

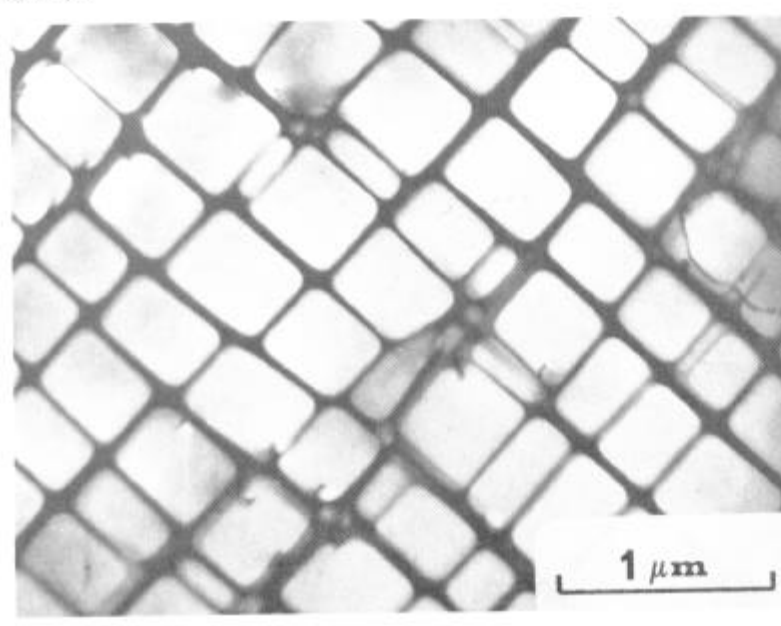


Figure 1: typical microstructure of the fully heat treated single crystal prior to creep test. (300) Dark field micrograph of a [001] foil.

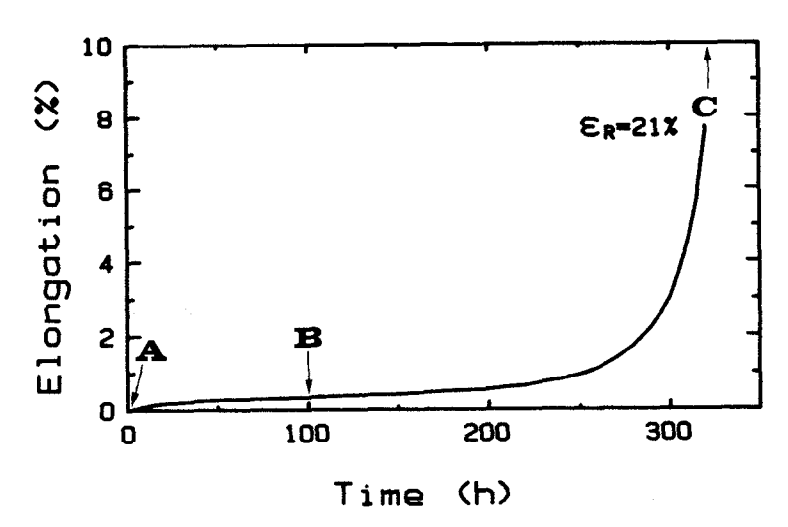


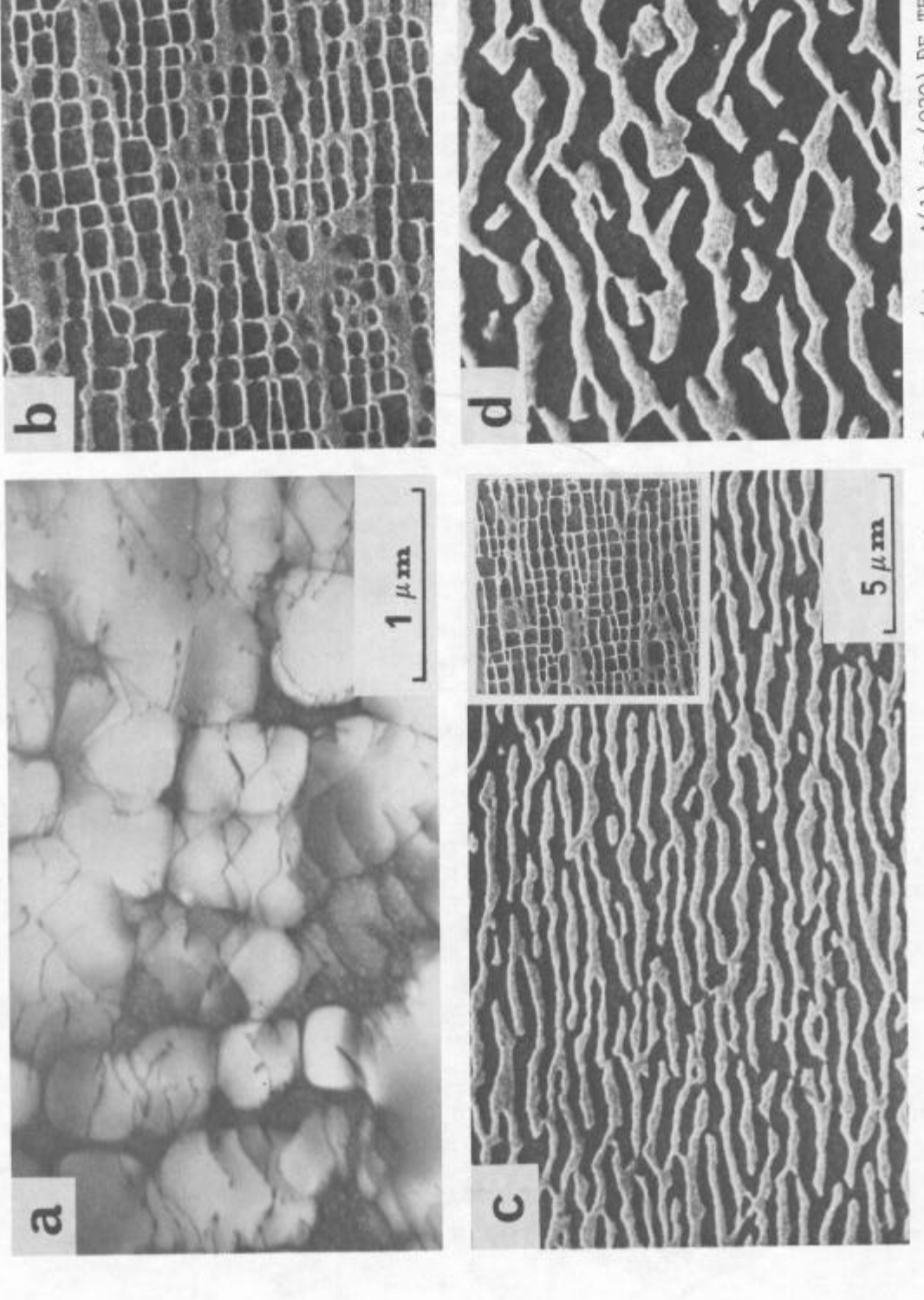
Figure 2: Creep curve obtained on the experimental alloy at 1050°C under 140 MPa.

Stage A: although the creep strain is still very small (0.02%) the lateral merging of the γ' cuboïds has already begun as observed by DF-TEM along the direction of the applied stress (fig. 3a). Notice that merging interfaces are usually deprived of dislocations. Looking at a longitudinal section by SEM (fig. 3b) confirms the tendency for vertical  $\gamma$  walls to become thinner, discontinuous or to disappear, and for horizontal walls to thicken sightly . No appreciable thickening of the  $\gamma'$  phase seems to have taken place. A thin foil normal to the [001] stress axis was examined under several diffracting conditions and Burgers vectors of the dislocations observed on figure 4 were determined. Burgers vectors  $\pm \frac{a}{2}$  [110] and  $\pm \frac{a}{2}$  [110] alone were missing although they could have appeared by recombination of the others. Almost all dislocations are lying in the (001)  $\gamma$ - $\gamma$ ' interfaces and along the [110] and [110] directions, thus forming about a 60° angle with their Burgers vector. Hence they tend to alleviate the misfit strain between the two phases but cannot do it as efficiently as pure edge dislocations. Their direction also indicates that glide is taking place on {111} planes in this alloy as reported by Caron and Kahn (9) in CMSX-2 and not on {110} planes as reported by Carry and Strudel (10) in alloy 01. Dislocations seemed to be confined to interfaces except for the leading screw segments, and nowhere did the  $\gamma^{\mbox{\tiny !}}$  seem to be sheared at this stage of the deformation process.

Stage B : After 100h the strain is only 0.35% but the lateral extension of the  $\gamma'$  phase is well under way as seen on figure 3c. Its thickness, as measured along the direction of the applied stress [001] has increased slightly ( $\simeq$  50%), but the striking point is the drastic thickening of the  $\gamma$  phase by a factor of 5 to 50, almost reaching a micron at places. Another novel feature of this structure is that  $\gamma$  is no longer continuous. Often it is now forming islands and is thus entirely surrounded by the  $\gamma'$  phase. This particular situation does not seem to impair creep resistance since the sample is only at one third of its creep life.

Stage C: Strain at rupture is very large (21%) but not very uniform along the gage length. Longitudinal sections taken away from the rupture surface exhibit features similar to those observed in stage B, only exagerated (fig. 3d). The  $\gamma$  phase is generally thicker than a micron, surrounded by the  $\gamma'$  phase and forming wavy and branching platelets. The  $\gamma$  phase has only thickened by a factor of 3 to 4 at most. The examination of thin foils reveals the presence of numerous dislocations in the  $\gamma'$  phase as reported in other alloys (9).

All these observations (fig. 3) describe the oriented coarsening of the alloy structure of type N and are in agreement with those made on U-700 (3).



insert at same maginification.d/stage C (330h, rupture) longitudinal with stress axi in (030) DF-TE Changes in microsctructure after various stages of creep.a/stage A(1) in (030) DF-T b/stage A in SEM on a [010] longitudinal section. c/stage B(100h) in a longitudinal elongated structure as in b and c. Figure

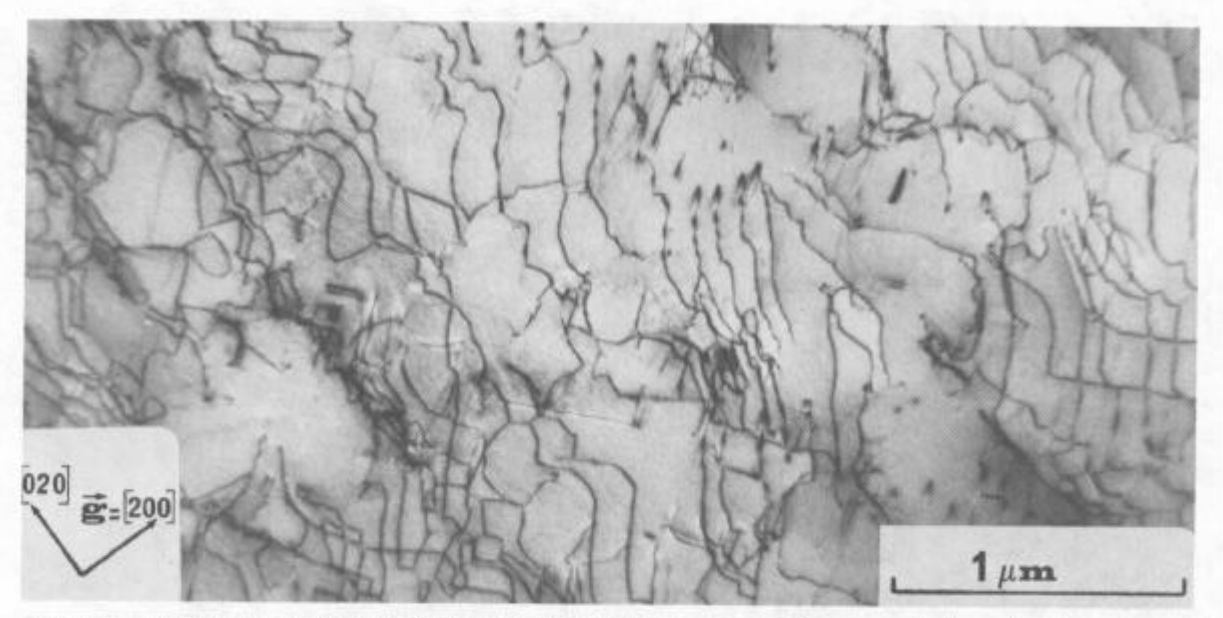


Figure 4: Dislocation structure in the initial stage of creep (stage A, 1h,  $\epsilon$ =0.02%)

Nasair 100 (5), CMSX-2 (9), MAR M200 (11) and alloy Ni-13 Al-9 Mo-2 Ta (4) but opposite to the type P behaviour observed on alloy 01 (7) and in the binary Ni-Al alloy (6).

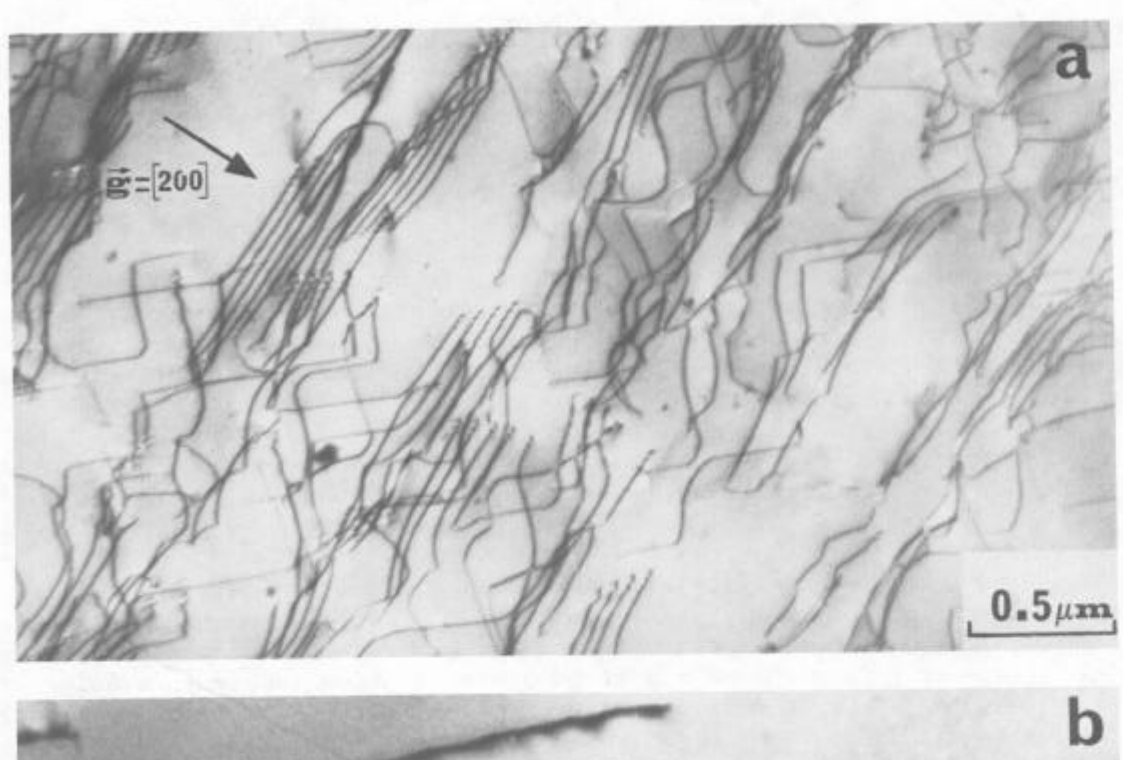
# Some Determinations of Misfit Parameters

In all three alloys studied here the growth of  $\gamma'$  precipitates larger than 1µm by long time ageing at 1050°C under no stress lead to the development of the interfacial dislocation networks. Depending on the dislocations readily available on the closest subgrain boundary, regularly spaced arrangements of parallel dislocations of one type have already developed after 200h in the experimental alloy as observed in thick regions by TEM at 300 kV (fig. 5a).

When examined under the g.b. = 2 diffracting conditions, so called "double images" or preferably asymetric images are formed (fig. 5b). Notice that the contrast profile of the interfacial dislocations is reversed on opposite sides of the \gamma' precipitate. Their inclination in the foil can be determined by inspection of a BF-DF pair of micrographs taken under same diffracting conditions: the "top end" of the dislocations located on the entrance side of the incident electron beam is identified by "in" on the micrograph (fig. 5b), the "bottom side" by "out". In contrast to the dislocations observed after 1h of creep at 1050°C (fig. 4), these lines are lying within 10 to 15° of a pure edge orientation. The results of the misfit amplitude and sign determinations are gathered in table I. The accuracy of these measurements is of the order of \$\frac{1}{2}.10^4\$ and is mainly limited by the irregularities observed in the dislocation spacings (fig. 5a)

Alloy	Alloy 01	CMSX-2	Experimental Alloy
Misfit $\delta = \frac{a_{\gamma'} - a_{\gamma}}{a_{\gamma}}$	+3,8 x 10 <sup>-3</sup>	-3,3 x 10 <sup>-3</sup>	-2,3 x 10 <sup>-3</sup>

Table I : In situ γ-γ' misfit parameter at 1050°C



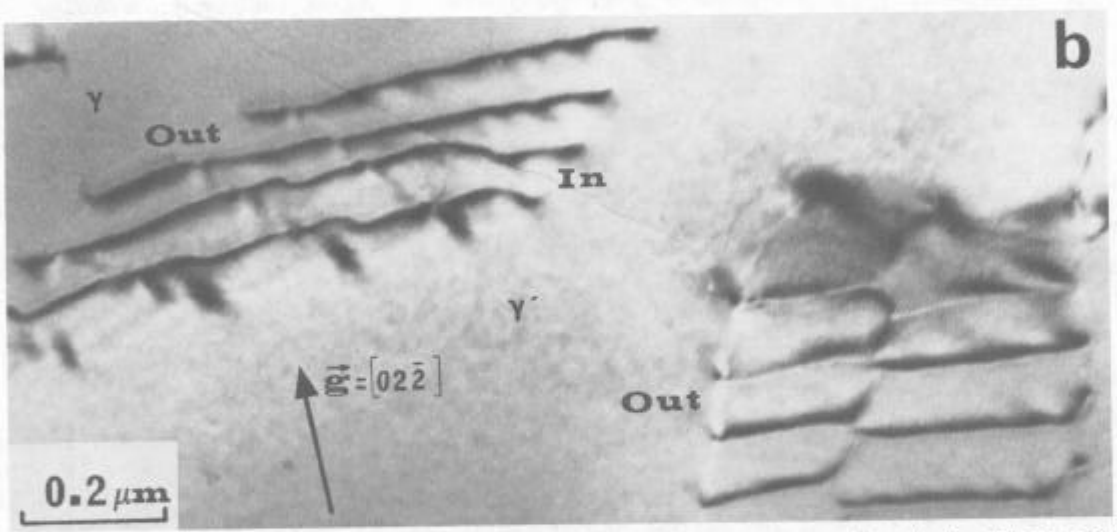


Figure 5: Interfacial dislocation arrangements in the experimental alloy after overageing without load at 1050°C, a) general view of inclined interfaces in a [110] foil observed at 300 kV (photo Duysen, EDF).
b) asymetric images observed under g.b. = 2 and w > 0 for the determination of the sign of δ.

A previous determination of the misfit parameter of alloy 01 (7) exhibited an erroneous sign probably originating from an incorrect sign convention used in TEM image simulation. Such errors can be avoided by direct reference to the kinematical schematic showing the respective positions of the core and of the image of the dislocation (12). The value of  $\delta$  for CMSX-2 at  $1050^{\circ}\text{C}$ :  $-3.3\times10^{-3}$  is different from the one measured by Caron and Khan (+ 1.4  $\times$   $10^{-3}$ ) (9) at room temperature. Similarly the determination of the room temperature misfit parameter of the experimental alloy by the convergent beam electron diffreaction (CBED) technique yields a value close to zero. These observations are consistent with the findings of Grose and Ansell (13) who report a general tendency for the misfit to decrease and become negative with rising temperature especially when  $\gamma'$  forming elements (Ti, Al, Nb) start disolving in the matrix and expand its lattice parameter.

#### Interpretation and Discussion

# Determination of the In Situ Misfit at Temperature

Two different techniques are currently used in order to evaluate misfit parameters of precipitation hardened alloys: CBED in TEM at room temperature (14) and high temperature X-ray techniques (13).

CBED techniques are more reliable than  $\delta$ -fringes techniques (8) but are necessarily limited to room temperature measurements. Holz-line broadening is quite apparent on diffraction micrographs of the  $\gamma$  phase strained by the overwhelming presence of the large cuboïds and of smaller  $\gamma'$  which precipitate during cooling to room temperature.

X-Ray techniques can be extended from room temperature up to  $800^{\circ}$ C but are limited by the diffuse thermal scattering which broardens the diffraction peaks (13).

The observation of equilibrium interfacial dislocation networks (2) is a reliable method for measuring the in situ misfit at the creep temperature which is the actual parameter that matters for understanding creep mechanisms and  $\gamma'$  coalescence, the relaxed misfit parameter at room temperature being of limited interest. This technique however is probably limited to higher temperatures only since Ostwald ripening of the  $\gamma'$  phase is considerably reduced as the ageing temperature is lowered : experiments are currently made on several alloys at 900°C for at least 1000h.

# Relationship Between $\delta$ and the Type of $\gamma^+$ Coalescence Observed

Oriented coarsening of the  $\gamma'$  phase during uniaxial creep tests at high temperature has been observed to follow two opposite patterns :

Type P Behaviour: platelets are formed which lie parallel to the tensile stress direction. In alloys with low f ( $\gamma$ ') strings of  $\gamma$ ' cubes aligned along <001> directions can form and rapidly turn into needles parallel to the applied tensile stress (6). In late stages or in alloys with larger f ( $\gamma$ '), two orthogonal sets of platelets parallel to  $\sigma$  are observed (7). The same type of structure is systematically observed after compressive tests in alloys exhibiting type N behaviour under tensile testing i.e. U-700 (3) and Nasair 100 (5) for instance.

The lattice misfit in the binary Ni-Al alloy is so strongly positive at room temperature that it is rather unlikely to decrease so much as to change sign before 750°C, the creep temperature used by Miyasaki et al (6). It can be estimated at  $\delta \simeq +~10^{-2}$  when taking a solubility limit of 10% at. Al at 750°C and a Vergard's coefficient of 1.71 x  $10^{-3}$ . Similarly alloy 01 actually exhibits a positive  $\delta$  at the creep temperature of 1050°C and follows identical coalescence patterns.

Type N Behaviour: "platelets" or "rafters" are formed which lie normal to the direction of the applied tensile stress. In alloys with large f ( $\gamma$ ') these platelets are either made by joining several adjacent  $\gamma$ ' cuboïds (at small strain) or formed by the thickening  $\gamma$  walls which rapidly turn into islands (starting at about 0.3 strain at 1050°C).

This structure elongated in the direction normal to the applied tensile stress is observed in a large number of recently developed nickel base superalloys designed for single crystal blades: Ni-Al-Mo-Ta alloys (4), NASAIR 100 (5), CMSX-2 (9), MAR-M 200 (11) and our experimental alloy (fig. 3). Type P structure is observed when the applied stress is of

compressive nature. Its appears to be generally associated with negative values of  $\delta$  at the creep temperature.

# Validity of the Elastic Model

The purely elastic model considered by Pineau (15) leads to the correct direction of the elongation of the structure if it assumed that the  $\gamma'$  phase is harder than the  $\gamma$  matrix (E ,>E ) at the creep temperature. This point has not received enough attention sofar and only Miyasaki et al(6) have established it clearly in the case of the Ni-Al alloy.

If such is also the case in the experimental alloy presented here, the purely elastic schematic of figure 6 would interprete correctly the lateral merging of  $\gamma'$  cubo described in figure 3a and suggest that stress oriented diffusion at 1050°C can modify the initial spacing of the  $\gamma'$  dispersion during the early stages of creep (stage A) even before the dislocations have reached their steady state density. Thinning of the  $\gamma$  walls parallel to the applied tensile stress and thickening of the horizontal walls would facilitate the movement of screw dislocations bowing between the cube faces normal to the stress direction.

The main role of the dislocations is to implement the shape transformation desirable elastically and convey the strain accross the structure. They are also quite likely to be used as short circuits for diffusion paths and are found to partially relax the misfit stresses on the cube faces normal to the applied stress.

The elastic model proposed by Pineau (15) must however be considered with caution since it is based on Eshelby's approach (16) which assumes that the precipitate is of small size and imbeded in a matrix of infinite size. The need for a more realistic model describing the case of  $f_{V}(\gamma')$  of the order of 60% to 70% is obvious.

# Matrix and Precipitates

In alloys with f  $(\gamma')$  > 50%, it is rather surprising to find the  $\gamma'$  phase still surrounded by the  $\gamma$  phase after heat treating : it is probably

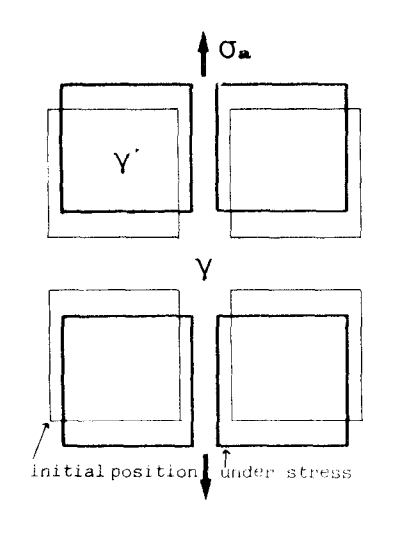


Figure 6 : Elastic model, hard γ' cuboïds in a soft matrix (E<sub>v'</sub>>>E<sub>v</sub>) under tensile stress.

due to the fact that the  $\gamma$  phase is the host phase since it is the phase forming at high temperature where the γ' nucleate during cooling. The  $\gamma-\gamma'$  interfacial energy may also contribute to maintain this situation in some alloys. But when strain deeply perturbs the structure at high temmperature, it is not too surprising to observe that the minor phase  $\gamma$ rapidly becomes surrounded by the major phase γ', thus decreasing the interfacial energy term. This process of  $\gamma-\gamma'$  inversion initiates quite early with creep strain and does not seem to deteriorate the creep resistance of the alloy, on the contrary. The elongated structure is perturbed by the plastic strain since shorter and thicker platelets are observed at rupture (fig. 3d) and the transformation of the  $\gamma$  phase into islands is more pronounced. Similar features can be observed in NASAIR 100 (5), CMSX-2 (9) and other alloys (4, 11) but have not been mentioned so far.

#### Conclusions

- 1- The in situ misfit at 1050°C has been estimated for several alloys and is generally negative in recently developed Ni base alloys, although it may be slightly positive at room temperature.
- 2- Two different patterns in  $\gamma'$  oriented coalescence are observed under tensile creep conditions: type P with plates parallel to the applied tensile stress is usually found in alloys with  $\delta\!>\!0$  and type N with plates normal to the tensile stress with  $\delta\!<\!0$ . This is consitent with the solutions of Pineau's model (15) when assuming that the elastic constants of the  $\gamma'$  phase are greater than in the  $\gamma$  phase (E  $_{\gamma'}$  > E  $_{\gamma}$ ).
- 3- Lateral merging of adjacent  $\gamma'$  cuboïds intitiates at an early stage of creep at  $1050^{\circ}\mathrm{C}$  (<1h) under 140 MPa and seems to precede dislocation multiplication. The formation of rafters does not seem to impair creep resistance in alloys capable of maintaining large  $f_{V}(\gamma')$  at the test temperature.
- 4- During creep at 1050°C glide on the <110>  $\{1\bar{1}1\}$  system was observed in the experimental alloy with  $\delta<0$  as in CMSX-2 (9) as opposed to the <110>  $\{1\bar{1}0\}$  system observed in alloy 01 (7) at 850°C (10).
- 5- In latter stages of creep, the thin walls of  $\gamma$  matrix ( $\approx$ 20nm) initially separating the  $\gamma'$  cuboïds either disappear when parallel to the applied stress or thicken by a factor of 5 to 50 ( $\approx$  600nm) when normal to the applied stress (type N coarsening behaviour). The  $\gamma$  phase is surrounding the  $\gamma'$  phase in the heat treated material prior to creep or after long time ageing with no applied stress. During creep,  $\gamma$  islands start forming within the first 10% of the creep life of the material and the  $\gamma$  phase appears to be generally surrounded by the  $\gamma'$  phase at rupture.

Further observations and measurements of  $\delta$ , E , E, in relation with rafting patterns are needed in order to identify clearly which of the observed features are beneficial and which are detrimental to alloy creep resistance.

### Acknowledgements

This work was supported in part by the Direction des Recherches et Etudes Techniques and in part by the Ecole Nationale Supérieure des Mines de Paris.

## References

- 1. Tsumuraya and Y. Miuata, Acta Metall., 31 (3) (1983), p 437.
- 2. A. Lasalmonie and J.L. Strudel, Philos. Mag., 32 (5) (1975) p 937.
- 3. J.K. Tien and R.P. Gamble, Metall. Trans., 3, (1972) p 2157.
- 4. D.D. Pearson, F.D. Lemkey and B.H. Kear, Proc. 4th Int. Symp. on Superalloys, Seven Springs, P.A., ASM, Metals Parc, OH, (1980) P 513.
- 5. M.V. Nathal and L.J. Ebert, Scripta Metall., 17 (9) (1983) p 1151.
- 6. T. Miyazaki, K. Nakamura and H. Mori, J. Mat. Sci. 14 (1979) p 1827.
- 7. C. Carry and J.L. Strudel, Acta Metall., 26 (1978) p 859.
- 8. J.M. Oblak and B.H. Kear, Trans. Quart. ASM, 61 (1968) p 519.
- 9. P. Caron and T. Khan, Mat. Sci. and Eng., 61 (1983) p 173.
- 10. C. Carry and J.L. Strudel, Scripta Metall., 9 (1975) p 731.
- 11. C.Carry, C.Houis and J.L.Strudel, Mem.Sci.Rev.Metall., 78 (1981), p.139.
- 12. A. Fredholm and J.L. Strudel, (unpublished).
- 13. D.A. Crose and G.S. Ansell, Met. Trans., 12A, (1981) p 1981.
- 14. R.A. Ricks, A.J. Porter and R.C. Ecob, Acta Metall., 31 (1983) P 43.
- 15. A. Pineau, Acta Metall., 24 (1976) p 559.
- 16. J.D. Eshelby, Progr. Solid. Mech., 2 (1961), p 87.